Indian Journal of Fibre & Textile Research
Vol. 48, June 2023, pp. 204-217
DOI: 10.56042/ijftr.v48i2.61188

Quantification of binder fibres in needle-punched nonwoven and its influence on physical-mechanical-functional properties of an air filter media

Rupayan Roy[1,2,a] , SM Ishtiaque[2], Animesh Laha[3], Shashi Sony[2]&Puneet Sood[1]

[1]Department of Fashion Technology, National Institute of Fashion Technology, Kannur 670562, India

[2]Department of Textile and Fibre Engineering, Indian Institute of Technology Delhi, New Delhi 110016, India

[3]Welspun India Limited, Senapati Bapat Marg, Lower Peral, Mumbai 400013, India

Received 31March 2022; revised received and accepted 4August 2022

A nonwoven filter (viscose fibres) with an optimal design has been developed by controlling the binder fibres (fibres in the vertical direction) in the needle-punched nonwoven. Box and Behnken design in conjunction with 3D surface analysis hasbeen used to study the effect of punch density, needle penetration depth and stroke frequency, considering the percentage of binder fibres in the overall structure on thickness, tenacity, air permeability and filtration efficiency of the filter. In this work, all the above properties are explained in the light of the considered structural index 'percentage of binder fibres'. It is observed that the percentage of binder fibres increases with the increase of all three considered punching parameters. The thickness and tenacity are found to be decreased and increased respectively, with the increase of binder fibre percentage. The air permeability initially decreases and then increases with the increase in the percentage of binder fibres, whereas the filtration efficiency showsthe opposite trend.

Keywords: Air filter, Air permeability, Binder fibres, Needle-punched nonwoven, Tenacity,Viscose fibre

1 Introduction

Nonwoven fabrics are the backbone of the technical textile sector. There are so many applications of nonwoven fabrics observed in the modern world. The nonwoven is mainly used as geo textiles to protect roads and river banks; filter media to protect humans from pollution (viruses, bacteria, water purification); medical devices to prepare different sensors, artificial body parts, disposable clothing; packaging as small carry bags to large-size food storage bags; and many other fields like automobile, construction and sports[1,2]. There are different types of nonwoven available for different end uses. Nonwovens are classified in terms of their manufacturing technology, such as needle punching, chemical bonding, thermal bonding, hydro-entanglement, etc.[3,4]. According to the current situation, industrial air filtration is a prime segment of the application of nonwoven, where needle-punched nonwoven fabrics are the principal material[5].

The production of needle-punched nonwoven fabrics, like the rest of textile production, has been backed mostly by empirical knowledge. Most of the research work explained the properties of a nonwoven based on variable parameters. In a study, Kothari *et al.*[6]studied the impact of layering in a composite nonwoven air filter produced with different needle punching parameters. They concluded that all properties are changing with changing the punch density up to a certain point. Anandjiwala *et al.*[7]conducted a study on the influence of variable machine parameters of a few needles-punched nonwoven fabrics prepared with different natural and manmade fibres. They noticed a significant impact of the process parameters on the physical-mechanical properties. Hearle *et al.*[8]concluded that the required fabric thickness and optimum packing density are controlled by the force applied to both surfaces of a nonwoven needle board. Interestingly, all the research works explained the relation between process parameters but ignored the fact of fibre orientation in the structure and its influence.

Recently, however, few theoretical studies have been accomplished to examine the relationship between the structure of nonwoven fabrics and their properties [9–15]. However, all those studies were done on only horizontal fibres, which are mainly governed by the carding parameters. Pourdeyhimi *et al.*[16] reported in one of their studies on the fibre length and orientation of fibres in nonwoven composites at

[a]Corresponding author.
E-mail: rupayan666@gmail.com

different needle punch densities with the help of an image analysis system for measurement. According to their conclusion, the fibre orientation becomes more random with the increase in needle punch density and at the same time, the mean fibre length was found to be reduced by up to 30%. Xu *et al.*[17] studied the structural characteristics of the fibre in nonwoven fabric by the technique of image analysis. This study utilised the simplified image of the nonwoven structure for image analysis, where it was considered a two-dimensional structure due to the very low thickness under consideration. The image was simplified with the help of the skeletonization algorithm developed by the authors. The structural characteristics like fibre length, fibre curl factor and fibre orientation were measured, considering them to be oriented and entangled to each other in the X-Y plane. This study claimed to be more comprehensive. Similarly, Hearle *et al.*[8,18] used a projection method for measuring the fibre orientation and fibre curl in the nonwoven structure. But these methods have a shortcoming in that it ignores the fact that the fibrous assembly is 3-dimensional,and the constituent fibres are distributed randomly in three planes (X, Y and Z).

Jeddi *et al.*[19] addressed the efficacy of optical Fourier transformation in determining the fibre orientation in fabrics. Finally, they concluded that the optical method is simpler, faster as well as more accurate and more suitable for both offline and online monitoring of fibre distribution. On the other hand, Boulay *et al.* [20]studied the orientation in a paper using the traditional technique of light scattering. The work done related to the characterization of the structure of nonwovens uses various methods based on flow field analysis, light scattering, and the Fast Fourier Transformation. Considering the work done by Pourdeyhimi *et al.*[21], in which a comparison was made between Fourier Transformation Analysis and Image Analysis, they concluded that Fourier Transformation analysis is more accurate and robust than the latter. The Fourier method can be used while dealing with hazy images of a sample with a very high basis weight.

From the above discussion, it is clear that all the attempted research work surprisingly ignored vertically oriented fibres or binder fibres. Therefore, well-organized research is required to understand the behaviour of the vertical fibres and their impact on the properties of needle-punched nonwoven. The barbed needles are used to punch the fibres inside the web structure and make the entanglement, which is mounted on a board. The punched fibres are oriented in a perpendicular direction to the carded webs. These vertically orientated fibres are defined as binder fibres by the authors in this article. Therefore, this research work is designed in such a way as to quantify the vertically oriented fibres or binder fibres as an effect of three considered punching parameters, viz. punch density, needle penetration depth and stroke frequency. The binder fibres are presented in terms of a percentage of the total fibres. The properties, such as thickness, tenacity, air permeability and filtration efficiency, are explained in the light of binder fibre percentage. Three-factors & three-level Box Behnken design is implemented for a more scientific assessment of the results and optimization of process parameters.

2Materials and Methods

2.1 Materials and Sample Preparation

The research work is commenced with the utilization of viscose fibres of staple length 38 mm1.5 denier. Actual values of variables corresponding to coded values are given in Table 1. A total of 15 samples were prepared as per the 3 factors 3 levels Box Behnken Design as shown in Table 2.

As per the response surface design, 15 sets of samples were prepared at a carding parameter of 0.180 m/min feeder speed, 175 m/min cylinder speed and 5.500 m/min doffer speed. The carded webs were needle punched only from the top side to prepare the fabrics. All the samples were prepared while keeping a basis weight of 200±10 gsm. The selected SEM images of nonwoven fabric are presented in Fig. 1.

2.2 Experimental Designs

The influence of machine parameters on the needle-punched nonwoven air filter fabric process was studied using a Box-Behnken design of three process factors, namely punch density (A), needle penetration depth (B), and stroke frequency (C), each being varied at three different levels. The levels of actual and coded factors are shown in Table 1. As shown in Table 2, the Box-Behnken design generated 15 experimental runs.

Table 1 — Actual values of variables corresponding to coded values

Variables	Coded levels		
	-1	0	+1
Punch density/cm^2 (A)	100	150	200
Needle penetration depth (B), mm	6	8	10
Stroke frequency/min (C)	100	200	300

Table 2 — Box Behnken design and the responses of physical and mechanical properties of nonwoven fabrics

Run	Punch density, cm^2 (A- Factor 1)	Needle penetration depth, mm (B- Factor 2)	Stroke frequency, permin (C- Factor 3)	Binder fibres, % (Response 1)	Thickness mm (Response 2)	Tenacity-machine direction, cN/tex (Response 3)	Tenacity-cross direction cN/tex (Response 4)	Air permeability $m^3/m^2/min$ (Response 5)	Filtration efficiency, %	
									3µm particles (Response 6)	5µm particles (Response 7)
1	150	10	300	4.83	2.1894	1.5335	0.2423	56.28	64	78
2	200	10	200	7.91	2.147	1.8828	0.2933	63.88	53	72
3	100	8	100	2.12	3.366	0.88984	0.1453	64.75	49	65
4	100	10	200	3.24	2.66	1.5116	0.2412	62.93	59	78
5	100	8	300	2.49	3.026	0.9423	0.1604	58.82	51	68
6	150	8	200	4.44	2.7455	1.4883	0.2266	51.39	68	83
7	150	8	200	4.53	2.7455	1.4627	0.2248	50.86	67	81
8	150	8	200	4.61	2.7455	1.4659	0.2287	53.77	67	82
9	200	8	100	6.29	2.7423	1.7767	0.2766	55.58	65	79
10	150	6	300	1.88	2.9548	1.2979	0.1789	60.24	61	73
11	150	6	100	1.71	3.2868	1.2397	0.1734	64.75	59	71
12	200	8	300	6.95	2.4653	1.8067	0.2836	57.82	66	80
13	150	10	100	4.88	2.4354	1.7061	0.2714	53.77	66	81
14	200	6	200	2.28	3.1255	1.3225	0.2658	54.15	64	80
15	100	6	200	1.52	3.667	0.7698	0.1516	65.97	47	67

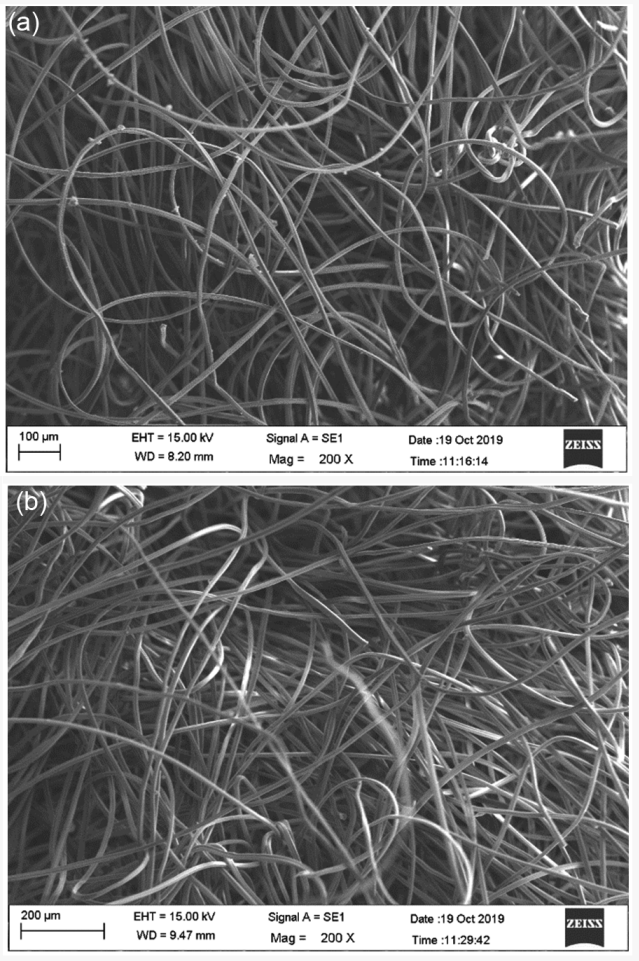

Fig. 1 — SEM images of the nonwoven fibrous network

The mathematical relationship between the response values (thickness, tenacity, air permeability& filtration efficiency) and the process variables can be described by the following nonlinear equation:

$$y = \beta_0 + \beta_1 X_1 + \beta_2 X_2 + \beta_3 X_3 + \beta_{12} X_1 X_2 + \beta_{13} X_1 X_3 + \beta_{23} X_2 X_3 + \beta_{11} X_1^2 + \beta_{22} X_2^2 + \beta_{33} X_3^2 + \varepsilon \quad \ldots (1)$$

where y denotes response values (thickness, tenacity, air permeability & filtration efficiency):X_1, X_2 *and* X_3indicate punch density, needle penetration depth and stroke frequency respectively;β_0 is constant, β_1, β_2, β_3 are linear coefficients;β_{11}, β_{22} and β_{33} are pure quadratic coefficients for punch density, needle penetration depth and stroke frequency respectively;β_{12}, β_{13} and β_{23} are mixed quadratic coefficients; and ε is the error term of the model. Design Expert 11 software was used to develop the equation and 3D surface plots.

2.3 Evaluation of Binder Fibre Percentage

To analyze the percentage of binder fibres (Z direction) in needled-punched nonwoven fabric, the carded webs of three different colours having a constant basis weight of 50 GSM were produced separately. The order of placement of the coloured and bottom-most grey fibre web is shown in Fig. 2(a). The samples were prepared as per the experimental design given in Table 2. The image colour summarization technique was used to measure the percentage of converted vertical as well as binder fibres that appeared on the bottom-most grey layer

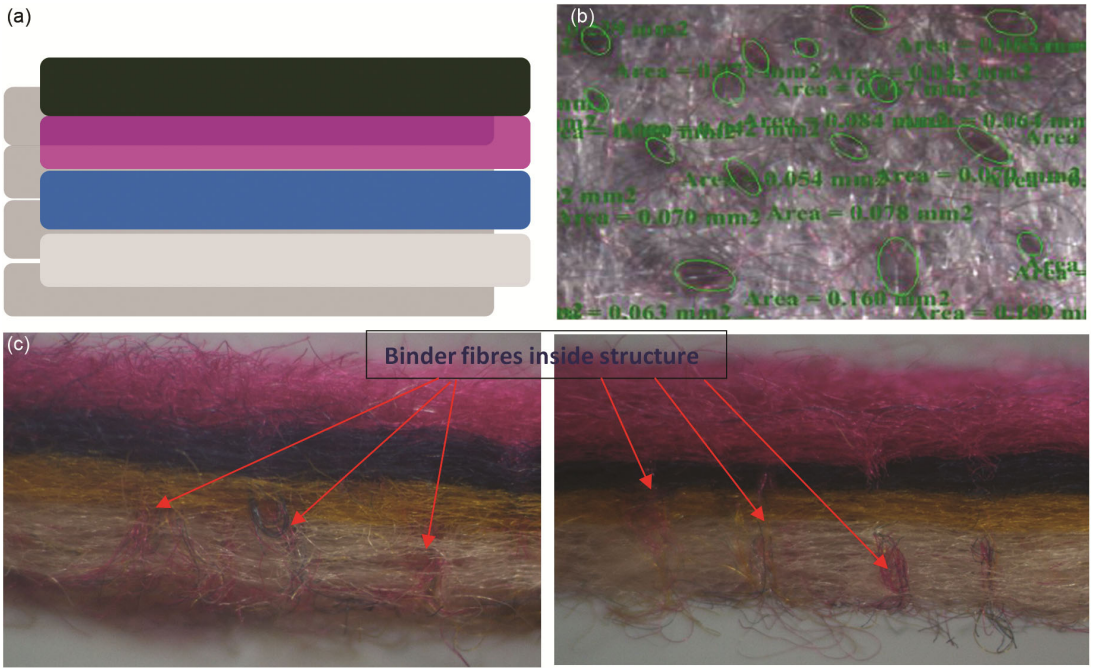

Fig. 2 — Evaluation of binder fibres percentage (a) sequence of layers of different coloured fibres, (b) binder fibres on a grey surface, and (c) cross-sectional view of nonwoven fabrics

due to needle punching. An optical microscope Nikon SMZ2500 with NIS Elements software was used to measure the percentage of binder fibres. The binder fibres on the grey surface and inside the structure are shown in Figs 2(b) and (c).

2.4 Evaluation of Mechanical and Functional Properties

The thickness of the fabrics was measured according to ASTM D1777-96 (2007) standard with the Essdiel thickness gauge at a pressure of 1.1 kPa. An average of 10 tests was taken into consideration. However, the evaluation of tensile strength was carried out in both machine and cross directions by using ZWICK/Roell Z100 as per ASTM D 5035. An average of five tests was taken into consideration. On the other hand, the air permeability of the fabric was measured using Textest FX 3300 air permeability tester at a pressure of 125Pa as per BS 5636. A sample size of ten was considered for air permeability measurement. The filtration efficiency and pressure drop of the nonwoven fabrics were measured by employing a purpose-built air filtration set-up, as discussed earlier[12].

3 Results and Discussion

3.1 Percentage of Binder Fibres

The variance analysis of the percentage of binder fibres is shown in Table 3 and the quadratic model is found to be significant. As shown in Table 3, the linear effects of punch density & needle penetration depth are statistically significant with p-value 0.0003 & 0.0004 on the percentage of binder fibres. The linear effect and square effect of stroke frequency also have some significant effects with a p-value of 0.017 and 0.022 respectively.

The response surface equations for the percentage of binder fibres in terms of coded factors and significant model terms are represented in the following equation:

$$\text{Percentage of binder fibres} = 24.6633 + 9.59 \times A + 9.17375 \times B + 0.79125 \times C + 5.325 \times AB - 5.24042 \times B^2 \quad \ldots (2)$$

Figure 3(a) shows the 3D surface plots of needle penetration depth *vs* punch density at a constant stroke frequency. The percentage of binder fibres increases with the increase of needle penetration depth and punch density at respective stroke frequency. The percentage of binder fibres increases with the increase of both punch density as well as needle penetration depth at a particular stroke frequency. But the increase of stroke frequency initially increases the binder fibre percentage, but higher stroke frequency slightly decreases the percentage of binder fibres at all combinations of punch density and needle penetration depth. The percentage of binder fibres increases with the increase of all three punching variables.

Table 3 — Variance analysis of percentage of binder fibres and fabric thickness

Source	Sum of squares	df	Mean square	F- value	p-value	Significance
			Percentage of binder fibres			
Model	1640.20	9	182.24	19.32	0.0023	Significant
Punch density (A)	735.74	1	735.74	77.98	0.0003	
Needle penetration depth (B)	673.26	1	673.26	71.36	0.0004	
Stroke frequency (C)	5.01	1	5.01	0.5308	0.4989	
AB	113.42	1	113.42	12.02	0.0179	
B^2	101.40	1	101.40	10.75	0.0220	
Residual	47.18	5	9.44	-	-	
Lack of fit	46.74	3	15.58	71.99	0.0137	Significant
Pure error	0.4329	2	0.2164	-	-	
Cor total	1687.38	14	-	-	-	
$R^2 = 0.9720$						
			Fabric thickness			
Model	2.54	9	0.2823	73.16	< 0.0001	Significant
Punch density(A)	0.6266	1	0.6266	162.40	< 0.0001	
Needle penetration depth (B)	1.62	1	1.62	420.40	< 0.0001	
Stroke frequency (C)	0.1785	1	0.1785	46.26	0.0010	
A^2	0.1053	1	0.1053	27.28	0.0034	
Residual	0.0193	5	0.0039	-	-	
Lack of fit	0.0193	3	0.0064	-	-	
Pure error	0.0000	2	0.0000	-	-	
Cor total	2.56	14	-	-	-	
$R^2 = 0.9925$						

The 3D surface plots of stroke frequency *vs* punch density at respective needle penetration depth is shown in Fig.3(b) The results show an increase in the percentage of binder fibres with the increase of stroke frequency and punch density at respective needle penetration depths. The increase of both stroke frequency and punch density increases the percentage of binder fibres at a particular needle penetration depth. It is further noticed that the increase of needle penetration depth increases the percentage of binder fibres at a different combination of punch density and stroke frequency but towards higher needle penetration depth, it slightly reduces at lower values of punch density and stroke frequency. But the increase of punch density, needle penetration depth and stroke frequency together enhance the percentage of binder fibres.

Figure3(c) shows the 3D surface plots of stroke frequency *vs* needle penetration depth at a constant punch density. An increasing trend of the percentage of binder fibres with the increase of stroke frequency and needle penetration depth at respective punch density is observed. The increase of both stroke frequency and needle penetration depth shows an initial increase and then a decrease in the percentage of binder fibres at lower punch density. But the percentage of binder fibres increases with the increase of punch density. It is interesting to note that with the increase of punch density, needle penetration depth and stroke frequency the value of the percentage of binder fibres increases.

The percentage of binder fibresrepresents the intensity of binder fibres in the z-direction. Thus, the more the fibres in the z-direction, the more will be the value of the percentage of binder fibres.Finally, punching parameters are optimised for the maximum value of the percentage of binder fibres in the layered fibrous web using Eq. (2). The combination of 9.962 mm needle penetration depth, 170.764 strokes/min (frequency) and 199.024 punches/cm^2 punch density provide an 8.015 % maximum value of the binder fibre percentage in the layered fibrous web.

3.2 Fabric Thickness

The variance analysis of fabric thickness is shown in Table 3 and the reduced quadratic model is found significant. The linear effect of punch density & needle penetration depth is observed as strongly significant with a p-value of <0.0001, whereas the linear effect of stroke frequency is also noticed as

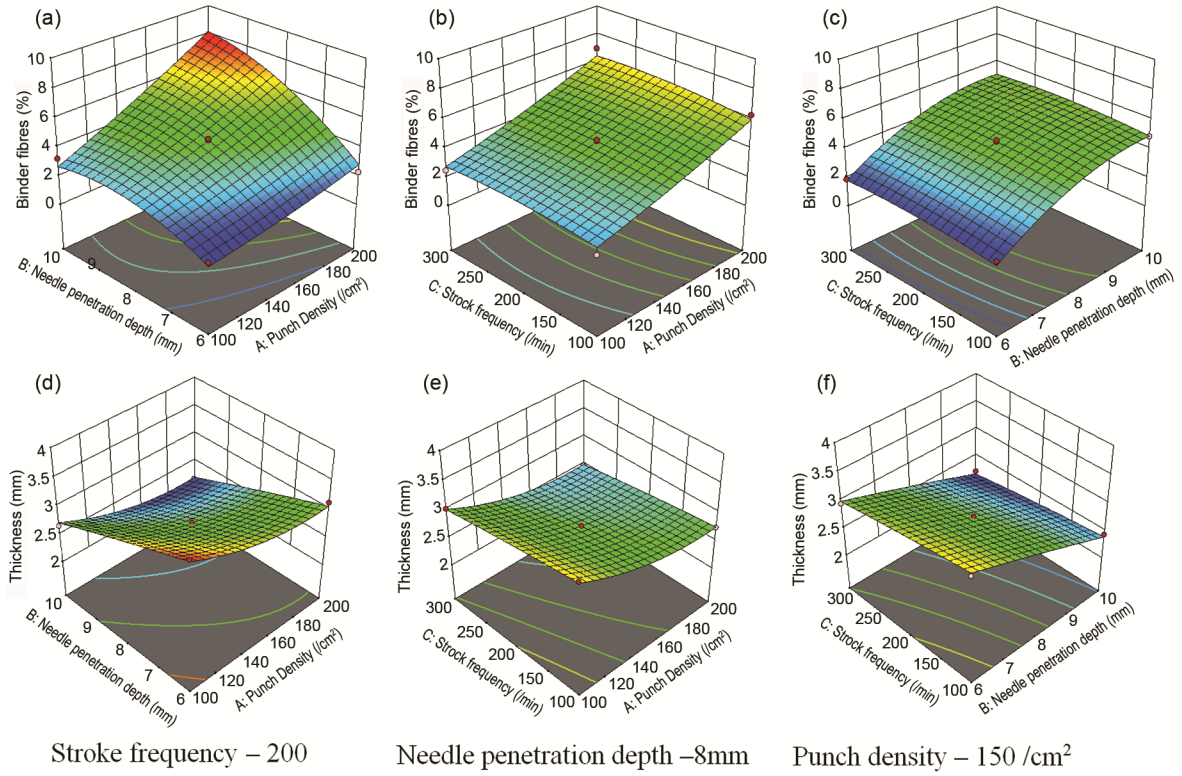

Fig. 3 — Influence of punching parameters on percentage of binder fibres (a-c), and fabric thickness (d-f)

significant with ap-value of 0.0010. The quadratic effect of punch density is observed as significant with a p-value of 0.0034.

The response surface equation for the fabric thickness in terms of coded factors and significant model terms is shown in the following equation:

$$\text{Thickness} = 2.7455 - 0.279862 \times A - 0.450288 \times B - 0.149375 \times C + 0.168838 \times A^2 \quad ...(3)$$

Figure 3(d) shows the 3D surface plots of needle penetration depth and punch density at constant stroke frequency. The fabric thickness decreases with the increase of needle penetration depth and punch density at respective stroke frequency. The results of fabric thickness show a decreasing trend with the increase of both punch density and needle penetration depth. The increase of stroke frequency shows a decrease in fabric thickness with the increase of both punch density and stroke frequency. Interestingly the fabric thickness shows a decreasing trend with the increase of punch density, needle penetration depth and stroke frequency together.

The 3D surface plots of stroke frequency and punch density at a constant needle penetration depth depict the decrease of fabric thickness with the increase of stroke frequency and punch density at respective needle penetration depth [Fig. 3 (e)]. The increase of both punch density and stroke frequency at a fixed needle penetration depth reduces the fabric thickness continuously. The increase of needle depth penetration shows a decrease in fabric thickness with the increase of both punch density and stroke frequency. However, the increase inpunch density, needle penetration depth and stroke frequency reduce the fabric thickness.

Figure 3(f) shows a reduction in fabric thickness with the increase of stroke frequency and needle penetration depth at a constant punch density. The increase of needle penetration depth, as well as stroke frequency at respective punch density, reduces fabric thickness and the increase of punch density continuously decreases the fabric thickness. But, the increase in punch density, needle penetration depth and stroke frequency shows a reduction in the fabric thickness.

As shown in Figs 3(d) –(f), the fabric thickness decreases as needle penetration depth and stroke frequency increase but increases with the increase of punch density. The decrease in fabric thickness is mainly due to the increase of fibre transfer in the z-direction, as explained above. Higher needle penetration depth and stroke frequency lead to an

Table 4 —Variance analysis of fabric tenacity in machine direction and cross direction

Source	Sum of Squares	df	Mean square	F-value	p-value	Significance
Machine direction						
Model	14184.19	6	2364.03	11.10	0.0017	Significant
Punch density(A)	8945.60	1	8945.60	41.99	0.0002	
Needle penetration depth (B)	5020.52	1	5020.52	23.56	0.0013	
Stroke frequency (C)	1.28	1	1.28	0.0060	0.9402	
Residual	1704.43	8	213.05	-	-	
Lack of fit	1700.53	6	283.42	145.67	0.0068	Significant
Pure error	3.89	2	1.95	-	-	
Cor total	15888.61	14	-	-	-	
R^2 = 0.8927						
Cross direction						
Model	331.09	6	55.18	16.11	0.0005	Significant
Punch density(A)	221.34	1	221.34	64.63	< 0.0001	
Needle penetration depth (B)	96.95	1	96.95	28.31	0.0007	
Stroke frequency (C)	0.0028	1	0.0028	0.0008	0.9778	
Residual	27.40	8	3.42	-	-	
Lack of fit	27.32	6	4.55	119.52	0.0083	Significant
Pure error	0.0762	2	0.0381	-	-	
Cor total	358.49	14	-	-	-	
R^2 = 0.9236						

increase in the percentage of binder fibres and the number of holes per unit area. This is responsible for more fibres in the vertical direction. On the other hand, with the increase of punch density, the fibres get spread towards the axis of the machine direction which also results in lower fabric thickness. But the results depict the reduction in the fabric thickness with the increase in punch density, needle penetration depth and stroke frequency.

Punching parameters are optimised for the maximum value of the thickness in the layered fibrous web using Eq. (3). The combination of 10 mm needle penetration depth, 291.559 strokes/min (frequency) and 200 punches/cm^2 punch density provide a 2.09 mm maximum value of the thickness in the layered fibrous web.

3.3 Fabric Tenacity in Machine Direction

The variance analysis of fabric tenacity in the machine direction is shown in Table 4 and the reduced quadratic model is found significant. The linear effect of punch density and needle penetration is noticed significant with a p-value of 0.0002 & 0.0013 respectively.

The response surface equation for the tenacity in machine direction in terms of coded factors and significant model terms is represented in following equation:

$$\text{Tenacity in machine direction} = 140.642 + 33.4395 \times A + 25.0512 \times B - 0.39925 \times C \quad ...(4)$$

The 3D surface plots of needle penetration depth and punch density at constant strokes frequency in the machine direction are given in Fig. 4(a). The results of fabric tenacity show an increasing trend with the increase of needle penetration and punch density at a respective stroke frequency. The results confirm the continuous increase in fabric tenacity at constant stroke frequency with the increase of both punch density and needle penetration depth. The increase of stroke frequency increases the fabric tenacity with the increase of both needle penetration depth and punch density but with the further increase of both needle penetration depth and punch density fabric, tenacity decreases. The increase of punch density, needle penetration depth and stroke frequency initially increase and then decreases the fabric tenacity.

The 3D surface plots of stroke frequency and punch density at a constant needle penetration depth of fabric tenacity in the machine direction are given in Fig.4(b). A continuous increase is observed with the increase of punch density and stroke frequency at a respective needle penetration depth. The increase of both stroke frequency and punch density shows an increasing trend at respective needle penetration depth, and the fabric tenacity also notices an increasing trend with the increase of needle penetration depth. The increase of punch density,

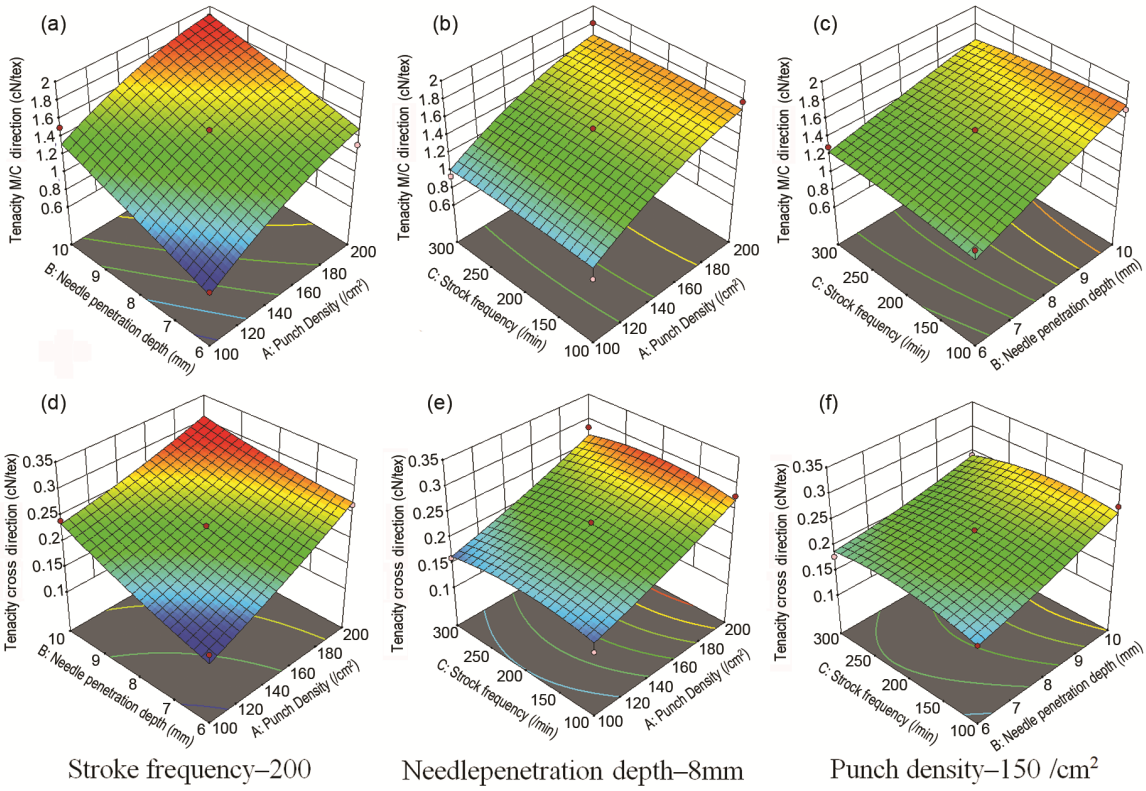

Fig. 4 — Influence of punching parameters on fabric tenacity in the machine direction (a-c), and cross direction (d-f)

needle penetration depth and stroke frequency increase the fabric tenacity.

Figure 4(c) shows the 3D surface plots of stroke frequency and needle penetration depth at a respective punch density of fabric tenacity in the machine direction. Fabric tenacity increases continuously with the increase of stroke frequency and needle penetration depth at respective punch density. The fabric tenacity notices an increase with the increase of both stroke frequency and needle penetration depth at a constant punch density and it also increases with the increase of punch density. The fabric tenacity shows an increasing trend with the increase of punch density, needle penetration depth and stroke frequency.

Punching parameters are optimised for the maximum value of the tenacity in the machine direction in the layered fibrous web using Eq. (4). The combination of 9.86 mm needle penetration depth, 116 strokes/min (frequency) and 200 punch/cm^2 punch density provide a 1.94 cN/tex maximum value of the tenacity in the machine direction.

3.4 Fabric Tenacity in Cross Direction

The variance analysis of tenacity in cross direction is shown in Table 4 and the linear model is found significant. The linear effect of punch density and needle penetration is found to be significant with a p-value of <0.0001 & 0.0007 respectively.

The response surface equation for the fabric Tenacity in cross direction in terms of coded factors and significant model terms is represented in the following equation:

$$\text{Fabric Tenacity in cross direction} = 22.426 + 5.26 \times A + 3.48125 \times B - 0.01875 \times C \quad ...(5)$$

Figure 4(d) shows that the fabric tenacity in cross direction increases with the increase of needle penetration depth and punch density at respective stroke frequency. The results of fabric tenacity in cross direction are identical to the results obtained in the machine direction but lower fabric tenacity in the cross direction.

The results of Fig. 4(e) show an increase in fabric tenacity in the cross direction with the increase of stroke frequency and punch density at a respective needle penetration depth. The trends of fabric tenacity in cross and machine directions are found to be identical. But the fabric tenacity in the machine direction is found to be lower in the cross direction.

Figure 4(f) shows the 3D surface plots of stroke frequency and needle penetration depth at constant punch density of fabric tenacity in the cross direction.

The trend of fabric tenacity obtained in machine and cross directions are similar, but fabric tenacity in the machine direction is always found to be lower.

It is observed from the response surface plots 4(a) -(f) that the tensile strength of nonwoven fabric in the machine direction and cross direction increases with the increase in the needle penetration depth and punch density but decreases with the increase in stroke frequency. The results have already established the increase of fabric tenacity with the increase of the punch density, needle penetration depth and stroke frequency. The increase in thepercentage of binder fibres, and the number of holes per unit area ensure more binder fibres with the increase of punch density, needle penetration depth and stroke frequency. This is responsible for the increase of fabric strength in the machine direction as well as cross direction.

The Eq. (5) of fabric tenacity in cross direction at a combination of 9.47 mm needle penetration depth, 146.476 strokes/min (frequency) and 200 punches/cm^2 punch density provide 0.312cN/tex maximum value of the tenacity in the cross direction.

3.5 Air Permeability

The variance analysis of air permeability is shown in Table 5and the reduced quadratic model is found to be significant. The linear effect of punch density is found to be significant as represented by the p-value of 0.05. The square effects of punch density, needle penetration depth & stroke frequency are also noticed as significant with a p-value of 0.0188, 0.0058 and 0.0459 respectively.

The response surface equation for air permeability in terms of coded factors and significant model terms is represented in the following equation:

$$\text{Air permeability} = 52.0067 - 2.63 \times A - 1.03125 \times B - 0.71125 \times C + 3.1925 \times AB + 2.0425 \times AC + 1.755 \times BC + 5.10417 \times A^2 + 4.62167 \times B^2 + 2.13167 \times C^2 \quad ...(6)$$

The results given in Fig. 5(a)show a reduction of air permeability with the increase of needle penetration depth and punch density at respective stroke frequency in the initial stage. Further increase of the two parameters increases the air permeability. It is noticed that stroke frequency of 100 strokes/min and 200

Table 5 —Variance analysis of air permeability

Source	Sum of squares	df	Mean square	F-value	p-value	Significance
Model	388.70	9	43.19	5.55	0.0363	Significant
Punch density (A)	41.89	1	41.89	5.39	0.0542	
Needle penetration depth (B)	10.25	1	10.25	1.32	0.3029	
Stroke frequency(C)	0.1996	1	0.1996	0.0257	0.8490	
A^2	88.51	1	88.51	11.38	0.0188	
B^2	180.31	1	180.31	23.18	0.0058	
C^2	63.12	1	63.12	8.11	0.0459	
Residual	38.90	5	7.78	-	-	
Lack of fit	33.70	3	11.23	4.32	0.1927	Not significant
Pure error	5.20	2	2.60	-	-	
Cor total	427.59	14	-	-	-	

R^2 = 0.9090

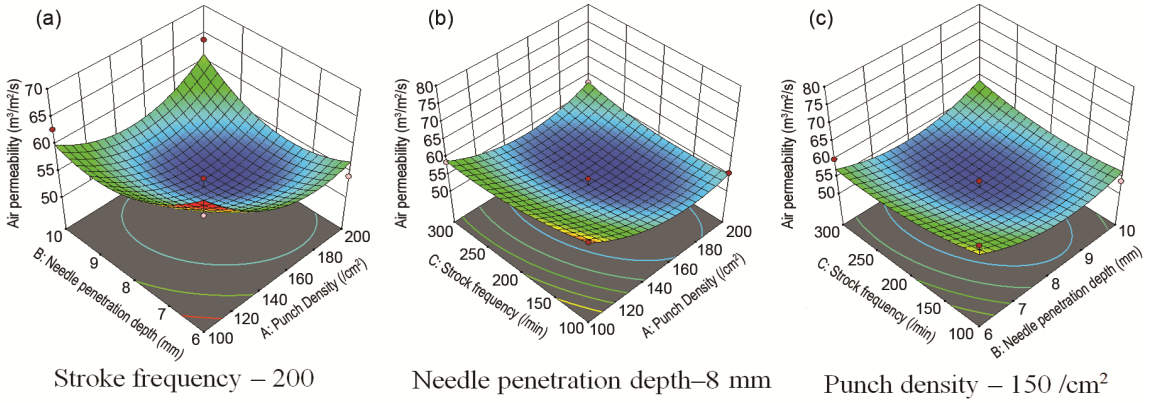

Stroke frequency – 200 Needle penetration depth–8 mm Punch density – 150 /cm^2

Fig. 5 — Influence of punching parameters on air permeability

strokes/min follow a decreasing trend but stroke frequency of 300 follows an increasing trend of air permeability with the increase of both punch density and stroke frequency. But the increase in stroke frequency reduces the value of air permeability, however, higher punch density and needle penetration depth show the opposite trend. Air permeability follows a decreasing trend with the increase of punch density, needle penetration depth and stroke frequency at the initial stage, thereafter the trend is reversed at the higher level of all three parameters.

The results of Fig. 5(b)show a decreasing and increasing trend in air permeability with the increase of stroke frequency and punch density at respective needle penetration depth. The air permeability reduces with the increase of both punch density and stroke frequency at 6mm needle penetration depth, but at 8 mm depth, it shows a slight increase and at 10 mm needle penetration depth a significant increase in air permeability is noticed. The increase of needle penetration depth notices a reduction in air permeability but an increase in air permeability at 150 punch density and 200 stroke frequency. The increase of punch density, needle penetration depth and stroke frequency initially reduces but after that increases the air permeability.

The results of air permeability given in Fig.5(c) indicate a reduction with the increase of needle penetration depth and needle penetration depth initial stage, beyond that air permeability and increases drastically at respective punch density. The air permeability initially decreases and then increases with the increase of both needle penetration depth and stroke frequency at respective punch density. But the increase of punch density increases the air permeability with the increase of both needle penetration depth and stroke frequency but towards a higher combination of punching parameters, it significantly increases the air permeability. The air permeability shows a decreasing and increasing trend with the increase of punch density, needle penetration depth and stroke frequency.

It is depicted in Figs 5(a) -(c) that air permeability initially decreases with the increase of needle penetration depth, stroke frequency and punch density but at later stage air permeability increases drastically. The above trend is found due to the changes that occurred in the percentage of binder fibres. The increase of the punching parameters increases the binder fibre quantity gradually. Interestingly, it is noticed that with the increase of binder fibre percentage, the air permeability is initially reduced but after a certain level, air permeability increases drastically with the increase of binder fibre percentage. The very high level of z-directional fibres or binder fibres promotes the generation of through pores, resulting in the easy passage of air to be passed through the filter fabric.

However, air permeability is very much dependent on fabric packing density which is inversely proportional to the thickness. As observed inFig.3, thickness shows a decreasing trend with the increase of needle penetration depth and stroke frequency. Therefore, the reasoning given above for fabric thickness supports the trend of air permeability with the increase of needle penetration depth and stroke frequency. The reverse trend isobserved for increasing punch density.

Punching parameters are optimised for the maximum value of the air permeability in the layered fibrous web using Eq. (6). The combination of 9.96 mm needle penetration depth, 298.589 strokes/min (frequency) and 200 punches/cm^2 punch density provide 66.116 m^3/m^2/m maximum value of the air permeability in the layered fibrous web.

3.6Filtration Efficiency of 3µmParticles

The variance analysis of filtration efficiency of 3µm particles is shown in Table 6 and the reduced quadratic model is found to be significant. The linear effects of punch density and needle penetration depth are found to be significant as represented by p-values 0.0019 & 0.0282. The interactive effect of needle penetration depth with punch density and the square effect of punch density is also found to be significant with a p-value of 0.022 & 0.0066 respectively.

The response surface equation for filtration efficiency of 3µm particles in terms of coded factors and significant model terms is represented in following equation:

$$\text{Filtration efficiency of 3µm particles} = 67.3333 + 5.25 \times A + 1.375 \times B + 0.375 \times C - 5.75 \times AB - 8.16667 \times A^2 \quad \ldots (7)$$

The 3D surface plots of needle penetration depth and punch density of filter efficiency at a respective stroke frequency are given in Fig. 6(a) and are represented by the response surface Eq. (7). The filtration efficiency for 3µm particles follows an increasing trend with the increase in needle penetration depth and punch density up to a certain

Table 6 — Variance analysis offiltration efficiency of 3µm and 5 µm particles (quadratic model)

Source	Sum of squares	df	Mean square	F- value	p-value	Significance
			3µm particles			
Model	649.68	9	72.19	5.83	0.0339	Significant
Punch density (A)	220.50	1	220.50	17.81	0.0196	
Needle penetration depth (B)	15.13	1	15.13	1.22	0.0282	
Stroke frequency (C)	1.13	1	1.13	0.0908	0.4223	
AB	132.25	1	132.25	10.68	0.0222	
A^2	246.26	1	246.26	19.89	0.0066	
Residual	61.92	5	12.38	-		
Lack of fit	61.25	3	20.42	61.25	0.0161	Significant
Pure error	0.6667	2	0.3333			
Cor total	711.60	14				
R^2=0.9130						
			5µm particles			
Model	173.14	9	16.13	16.27	0.0039	Significant
Punch density (A)	20.55	1	20.55	19.35	0.0079	
Needle penetration depth (B)	24.56	1	24.56	20.25	0.0084	
Stroke frequency (C)	3.13	1	3.13	0.1524	0.6856	
AB	90.25	1	90.25	6.61	0.0500	
A^2	101.77	1	101.77	7.46	0.0413	
Residual	68.25	5	13.65			
Lack of fit	66.25	3	22.08	22.08	0.0436	Significant
Pure error	2.00	2	1.0000			
Cor total	499.73	14				
R^2=0.8634						

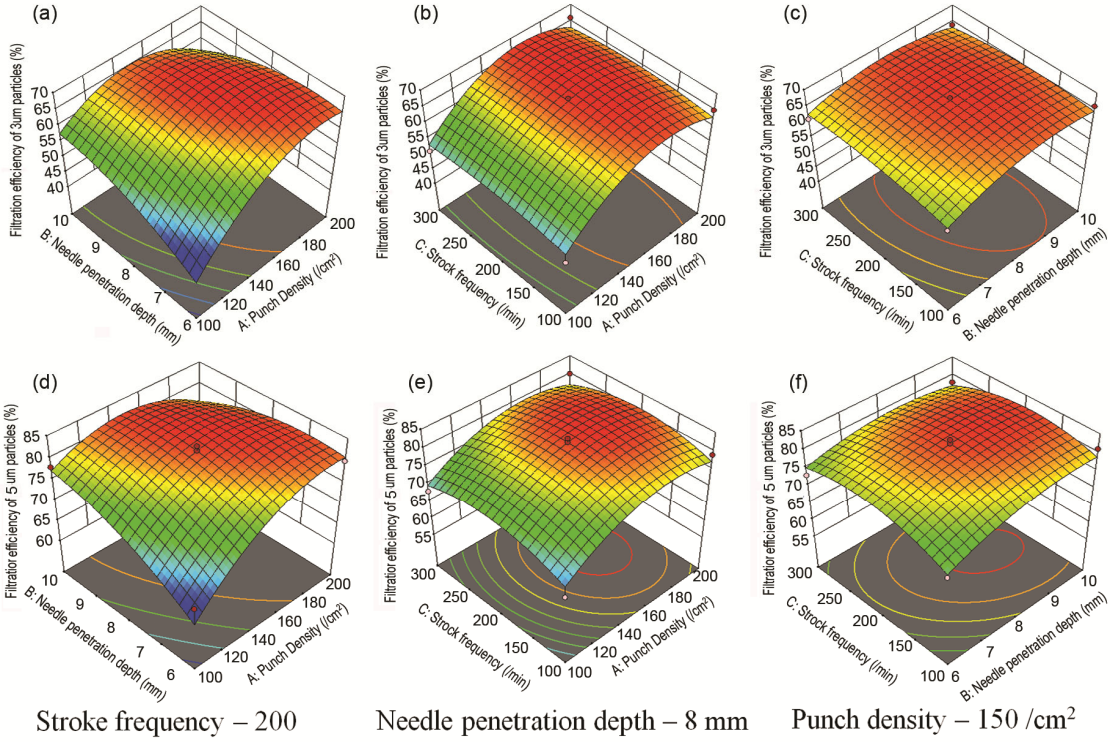

Fig. 6 — Influence of punching parameters on the filtration efficiency of 3µm particles(a-c), and 5 µm particles(d-f)

limit at respective stroke frequency. The filtration efficiency is increased with the increase in both punch density and needle penetration depth initially, thereafter reduction occurs towards higher values of needle penetration depth and punch density at respective stroke frequency. But the filtration efficiency follows an initial increase and then decreases with the increase in stroke frequency. The filtration efficiency for 3µm particles show an increasing trend with the increase in punch density, needle penetration depth and stroke frequency up to a certain limit, but towards higher punching combinations the reverse trend is observed.

Figure6(b)shows the 3D surface plots of stroke frequency and punch density at constant needle penetration depth. The filtration efficiency of 3µm particles increases with the increase in stroke frequency and shows a reduction towards higher stroke frequency and punch density at respective needle penetration depths. The increase in both punch density and stroke frequency at respective needle penetration depth shows an initial increase and then a decrease in the filtration efficiency. But the increasein needle penetration depth depicted a contentious increase towards lower values of stroke frequency and punch density and then it follows an increasing and decreasing trend of filtration efficiency. The filtration efficiency of 3µm particles shows an increase and then decreases with the increase in punch density, needle penetration depth and stroke frequency.

The 3D surface plots of stroke frequency and needle penetration depth at a fixed punch density of filtration efficiency of 3µm particles are given in Fig.6(c). The filtration efficiency depicts an increase and then decreases with the increase in stroke frequency and needle penetration depth at respective punch density. The increase in both needle penetration depth and stroke frequency at respective punch density shows an increase, but towards higher values of stroke frequency and needle penetration depth, the filtration efficiency shows a declining trend. But the increase in punch density also shows an increase and then a decrease in filtration efficiency. The increase in all three punching parameters follows an increasing and then decreasing trend of filtration efficiency.

The filtration efficiency of 3µm particles is optimized for maximum value using Eq. (7). The combination of 6.638 mm needle penetration depth, 228.505 strokes/min (frequency) and 200 punches/cm^2 punch density provides 65.926 % of the filtration efficiency of 3µm particles.

3.7Filtration Efficiency of 5µmParticles

The variance analysis of the filtration efficiency of 5µm particles is shown in Table 6 and the reduced quadratic model is found significant. The linear effects of punch density and needle penetration depth are found to be significant as represented by p-values 0.0079 & 0.0084. The interactive effect of needle penetration depth with punch density and the square effect of punch density is also found to be significant with a p-value of 0.05 & 0.0413.

The response surface equation for filtration efficiency of 5µm particles in terms of coded factors and significant model terms is represented in the following equation:

$$\text{Filtration efficiency of 5µm particles} = 82 + 4.125 \times A + 2.25 \times B + 0.375 \times C - 4.75 \times AB - 5.25 \times A^2 \quad \ldots (8)$$

Figure6(d) shows the 3D surface plots of needle penetration depth and punch density at a fixed stroke frequency. It is observed that trends of filtration efficiency of 5µm particles for all experimental combinations are identical to 3µm particles as discussed above, but the filtration efficiency of 5µm particles is found to be higher than that of 3µm particle size.

Figure6(e) shows the 3D surface plot of stroke frequency and punch density at a respective needle penetration depth. It is observed that trends of filtration efficiency of 5µm particles for all experimental combinations are identical to 3µm particles as discussed above but are higher in terms of filtration efficiency value.

Figure6(f) showed the 3D surface plot of stroke frequency and needle penetration depth at a constant punch density. The trends of filtration efficiency of 5µm particles for all experimental combinations are found to be identical to 3µm particles as discussed above, but provide a higher value of filtration efficiency in comparison to 3µm particle size.

The filtration efficiency of 5µm particles is optimized for maximum value using Eq. (8). The combination of 6.965 mm needle penetration depth, 207.052 strokes/min (frequency) and 200 punches/cm^2 punch density provide 81.517 % filtration efficiency of 5µm particles.

It is observed from the results that filtration efficiency follows initially an increasing trend with

Table 7 — Goals set for optimization process

Parameter	Goal	Lower	Upper	Lower weight	Upper weight	Importance
Punch density (A)	In range	100	200	1	1	3
Needle penetration depth (B)	In range	6	10	1	1	3
Stroke frequency (C)	In range	100	300	1	1	3
Air permeability	Maximize	50.86	65.97	1	1	5
Filtration efficiency of 3µm particles	Maximize	47	68	1	1	5
Filtration efficiency of 5µm particles	Maximize	65	83	1	1	5

the increase in needle penetration depth, stroke frequency and punch density at a lower level of punching parameters, but towards higher punching intensity a reducing trend of filtration efficiency is noticed. The observed trends are valid for both considered sizes of particles but the filtration efficiency of 5µm particles is found to be higher. Filtration efficiency is a dependent variable of thickness and air permeability of nonwoven fabrics. In an earlier discussion, it has been established that the thickness and air permeability follow a decreasing and then increasing trend, but the fabric thickness depicts a continuous decrease with the increase of punch density, needle penetration depth and stroke frequency. Hence, it is confirmed that mean flow pore size and air permeability follow the reverse trend of filtration.Thelower the meanflow pore size and air permeability, the higher is the filtration efficiency.

3.8 Optimization of Process Parameters

The optimization process has been carried out to obtain a filter media with maximum filtration efficiency with possible higher air permeability. Comparatively higher importance is given to the filtration efficiency of 3µm and 5µm particles as shown in Table 7.

The optimized process parameters and the related properties are given below:

Parameter	**:**	**Value**
Punch density/cm^2	:	198.470
Needle penetration depth,mm	:	6.600
Stroke frequency/min	:	264.618
Air permeability, m^3/m^2/min	:	58.335
Filtration efficiency of 3 µm particles, %	:	63.192
Filtration efficiency of 5 µm particles, %	:	78.737
Desirability	:	0.663

A lower order of penetration depth along with a higher order of punch density and stroke frequency is found as an optimized point as per required goals.

4 Conclusion

The above discussion concludes that the physical-mechanical properties of nonwoven are very much dependent on the proposed index percentage of binder fibres). It is observed that the percentage of binder fibres depicts an increase with the increase in punch density, needle penetration depth and stroke frequency. On the other hand, fabric thickness follows a decrease and bursting strength shows an increase with the increase of all considered punching parameters. The fabric tenacity in both directions is found to be increased with the increase of punching parameters. Further, it is noticed that the air permeability follows an initial decrease and then increases, whereas the filtration efficiency initially increases and then decreases with the increase of punching parameters.

Therefore, it can be summarized that the thickness continuously decreases and tenacity in both directions continuously increases with the increase in the percentage of binder fibres. However, the air permeability initially decreases and then drastically increases with the increase in the percentage of binder fibres but interestingly the filtration efficiency follows an opposite trend of air permeability.

References

1 Horrocks A R & Anand S C, *Handbook of Technical Textiles* (Elsevier) 2000.
2 Paul R, *High Performance Technical Textiles* (John Wiley & Sons)2019.
3 Kellie G, *Advances in Technical Nonwovens* (Woodhead Publishing) 2016.
4 Banerjee P K, *Principles of Fabric Formation* (CRC Press) 2014.
5 Maduna L& Patnaik A, *Text Prog*, 49 (4)(2017) 173.
6 Kothari V K, Das A & Sarkar A, *Indian J Fibre Text Res,* 32 (2)(2007) 196.
7 Anandjiwala R D & Boguslavsky L, *Tex Res J*, 78 (8) (2008) 614.
8 Hearle J W S & Stevenson P J, *Text Res J*, 33 (11) (1963) 877.
9 Thibault X & Bloch JF, *Text Res J*, 72 (6)(2002) 480.
10 Roy R& Ishtiaque S M, *Fibers Polym*, 20 (1) (2019) 191.
11 Roy R, Ishtiaque S & Dixit P, *J Ind Text*, 18 (2020).https://doi.org/10.1177/1528083720910706.

12 Dixit P, Ishtiaque S M & Roy R, *Compos Part B Eng*, 182 (2020).https://doi.org/10.1016/j.compositesb.2019.107654
13 Roy R, Chatterjee M & Ishtiaque S M, *Fibers Polym*, 21 (1) (2020) 188.
14 Roy R & Ishtiaque S M, *Indian J Fibre Text Res*, 44 (2)(2019) 131.
15 Roy R & Ishtiaque S M, *Indian J Fibre Text Res,* 44 (3) (2019) 321.
16 Pourdeyhimi B, Ramanathan R & Dent R, *Text Res J*, 66 (12)(1996) 747.
17 Bugao X& Ting YL, *Text Res J*, 65(1) (1995) 41.
18 Hearle J W S & Stevenson P J, *Text Res J*, 34 (3) (1964) 181.
19 Jeddi A A, Kim H & Pourdeyhimi B, *Int Nonwovens J*, 10 (2001) 10.
20 Boulay R, Drouin B, Gagnon R & Bernard P, *J Pulp Pap Sci*, 12 (1)(1986) J26.
21 Pourdeyhimi B, Dent R & Davis H, *Text Res J*, 67 (2) (1997) 143.